ASSESSMENT OF VIBRATION ISOLATION GENERATED BY THE INERTIAL FORCES OF AN AIRCRAFT COMBUSTION ENGINE ON A TEST BENCH

Grzegorz M. SZYMAŃSKI [1, *] ⓘ **, Marek WALIGÓRSKI** [2] ⓘ **, Wojciech MISZTAL** [2] ⓘ

[1] Poznan University of Technology, Institute of Transport,
[2] Poznan University of Technology, Institute of Combustion Engines and Powertrains,
* Corresponding author, e-mail: grzegorz.m.szymanski@put.poznan.pl

Abstract

The scientific issues that are the subject of this article are related to the assessment of the vibration damping efficiency of an aircraft engine installed on a test stand for the type of vibration isolator used. For this purpose, appropriate empirical tests were carried out on an aircraft internal combustion piston engine of the Rotax 912 type, under conditions of variable engine speed, for selected mounting locations of vibration transducers on the engine and its frame. The effectiveness of vibration isolation of vibrations generated by inertia forces was assessed, based on the proposed mathematical equations and the determination of the values of discrete impulse and energy measures describing them for accelerations, velocities and vibration displacements in various directions. Thanks to this, it became possible to perform a diagnostic assessment of the generation and propagation of vibrations and their isolation from the perspective of operational vibration loads on the object and its supporting structure, as well as in the context of the research reliability of the signal for a given type of damping of forces and moments of inertia.

Keywords: order analysis, vibration isolation, empirical research, aircraft engine, susceptibility method

List of Symbols/Acronyms

A	amplitude
a_1	vibration accelerations obtained from the transducer placed at the engine block
a_2	vibration accelerations obtained from the transducer placed at the engine frame
$a_{i, block}$	vibration accelerations in i (X, Y, Z) direction at the engine block
$a_{i, frame}$	vibration accelerations in i (X, Y, Z) direction at the engine frame
β	machine susceptibility
c	attenuation
δ	susceptibility of the frame structure
E_F	efficiency of force vibration isolation
E_x	efficiency of displacement vibration isolation
F(t)	value of the force from the source of excitation
FFT	Fast Fourier Transform
φ	phase shift angle
F_o	static force
G_e	stream mass of fuel consumption
γ	vibration isolator susceptibility
IC	internal combustion
k	stiffness
ξ	non-dimensional attenuation coefficient
m	mass
n	engine crankshaft speed
p	forcing frequency

p_o	ambient pressure
R(t)	force transferred to the supporting structure for the system with a vibroisolator (value after passing through the isolator),
RMS	Root Mean Square
SD	Secure Digital
t	time
T	torque
TEDS	Transducer Electronic Datasheet
t_o	ambient temperature
U	voltage
x(t)	displacement for a system without a vibration isolator
z(t)	displacement for a system with a vibroisolator (after passing through the vibroisolator)
$z_o(t)$	displacement of a system after a vibration vibroisolator in the conditions of a static force

1. INTRODUCTION

Order Analysis based on the FFT analysis is used when only lower orders are of interest, orders are well separated, rotational speed variation is limited, processing resources are scarce. In the case of the order tracking high orders are of interest and when rotational speed variation is wide and or fast. FFT spectra and slices are shown as function of rotational speed measured by the tachometer in the case of the order analysis based on the FFT (low cost, on-line analysis,

slice extraction with multiple tacho references). The above method is limited by smearing of higher orders, it is only for lower, well separated orders over a limited speed range. In the order tracking, the frequency range of an order analyzer changes in accordance with the rotational speed of the machine under investigation. The result is that individual orders remain on the same order line on the plot and smearing is avoided. In the above technique close orders and very high orders can be identified and analyzed.

Advanced measurement procedures to which objects with high variability of working processes occurring in them and the interdependence of their various origins and nature of course on the resulting signals obtained from them require detailed knowledge of each of them and the functional relations describing them. Thanks to this, there is obtained not only a faithful picture of the operating and operational characteristics for stationary and non-stationary conditions of use, but also the changes that occur in them under the influence of time and intensity of use. The specific knowledge base is then enriched by data obtained as a result of modifying geometrical and material characteristics or control variables, which are the basis for inferring the possibility of improving the object within its design limitations. The overall efficiency of the tested system is then determined on the basis of the relationship between the fidelity of mapping the dynamic main processes in the measurement signal waveforms, from which diagnostic parameters are obtained in the form of time histograms. Quantitative assessment of an object and changes occurring in it is possible when these process measures are reliable and have a sufficiently high active value of the signal describing the source process [3, 23, 24, 26]. The above uniqueness of the equations describing the source process provides the basis for further forecasting changes in the system's operating characteristics over time at a given intensity of use, the more significant the more accurate the mapping [2, 13, 18, 25]. As a result of specific analyses, a multidimensional space of discrete quantities describing the course of thermodynamic processes in the machine is obtained, taking into account their nature and genesis.

The basic condition for obtaining reliable measurement signals from the tested object is a clear relationship between the observed dynamic process and the physical quantities selected for its assessment. The more faithful the representation of this function, the better the mathematical description of process changes and their nature [10, 14, 21]. As a result, the multidimensional description of the genesis and behavior of the object in the conditions of its actual working environment becomes more complete, showing real possibilities of influencing the object in order to achieve greater overall efficiency. This approach to system analysis is even more expected the more often measures obtained from observations of accompanying processes are used in diagnostic assessment, such as in the case of vibroacoustic signals [16, 19, 20, 22].

However, before measurements are taken, it is paramount to ensure the appropriate quality of the object's foundation on the test stand. Knowledge of the forces and moments generated in the system and their energy propagation outside its structure allows for appropriate damping of their amplitude to minimize their impact on the supporting structure, foundation and surrounding objects. Thanks to this, their influence on the reaction to excitations is also minimized, which ensures obtaining a greater information value of the signal, the greater the complexity of the structure of the object and the correlation between the parameters. Appropriate vibration isolation also has a beneficial effect on the level of system safety, reflected in safety performance indicators, which is particularly important for air transport [11].

In order to reduce the value of the vibration amplitudes of the object due to internal and external forces, appropriate tools should be used to limit the displacements between the source and the energy absorbing system [4]. The above element or system is a vibration isolator and the phenomenon itself is called vibration isolation. Linearity and stationarity are assumed when modeling objects with mechanical vibrations generated in them. Then the processes implemented in them are treated as determined or stationary random. The evaluation of the excitations and their mathematical description is then carried out using the frequency domain and in the area of system properties based on transmittances as system characteristics regarding a susceptibility.

In real cases, the connections between the vibration source, the insulator and the energy receiver are multi-point or surface-based, hence the modeling apply to extended finite systems or discrete matrix models. Reduction of vibration amplitudes is achieved by separating dynamic forces from an isolated area (force vibration isolation) or dynamic displacements of a vibration-sensitive system (displacement vibration isolation) [12].

A dynamic process carried out in an object generating mechanical vibrations creates a dynamic force. The machine is placed on a supporting structure. If the permissible vibration amplitudes are exceeded, the source is excessive resultant dynamic force and incorrect selection of subsystem properties (source, isolator, vibration receiver). Reducing this force is possible by comparing the dynamic system without and with a vibration damper, using a susceptibility matrix (Fig. 1−2).
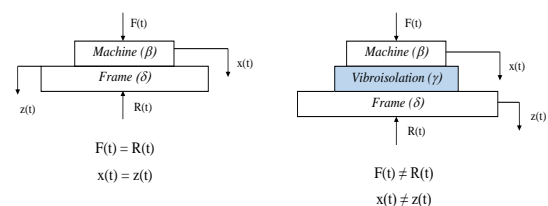

Fig. 1. Idea of using vibration isolation and the relationship between forces and displacements for the system without and with an isolator
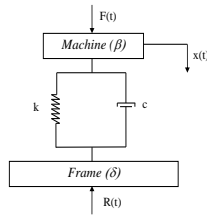
Fig. 2. Definition of a force vibration isolation [12]

The value of the force R(t) as a response to excitations originating from dynamic processes occurring in the machine is the sum of the product of the displacement and stiffness of the system as well as the speed and damping coefficient, according to the relationship:

$$R(t) = kx(t) + c\frac{dx}{dt}, \qquad (1)$$

The value of the vibration amplitude transmitted to the engine frame structure in force vibration isolation should be much smaller than the values generated as a result of excitations from dynamic processes occurring in the facility:

$$\sup[R(t)] \ll \sup[F(t)], \qquad (2)$$

The equation describing the dynamic interactions for a system with force vibration isolation is described by the following relationships:

$$m\frac{d^2x}{dt^2} + c\frac{dx}{dt} + kx = F_o\cos(pt), \qquad (3)$$

$$x(t) = A\cos(pt - \varphi), \qquad (4)$$

where:
m − mass,
c − attenuation,
k − stiffness,
F_o − static force,
A − amplitude,
p − forcing frequency,
t − time,
φ − phase shift angle.

The value of vibration insulation effectiveness is described using the following relationship [12]:

$$E_{F,x} = \frac{[F(t)]_{max}}{[R(t)]_{max}} = \frac{[z(t)]_{max}}{[x(t)]_{max}} \gg 1, \qquad (5)$$

where:
F(t) − force transmitted to the supporting structure for the system without a vibration isolator,
R(t) − force transferred to the supporting structure for the system with a vibroisolator (value after passing through the isolator),
x(t) − displacement for a system without a vibration isolator,
z(t) − displacement for a system with a vibroisolator (after passing through the vibroisolator).

As a result of transforming equation (1), taking into account dependencies (3) and (4), the following equations will be obtained:

$$R(t) = kx(t) + c\frac{dx}{dt} = A\big(k\cos(pt - \varphi) - cp\sin(pt - \varphi)\big) = R_o\cos(pt - \varphi + \alpha) = R_o\cos(pt - \varphi)\cos(\alpha) - R_o\sin(pt - \varphi)\sin(\alpha), \qquad (6)$$

Considering that:

$$R_o\cos(\alpha) = Ak, \qquad (7)$$

$$R_o\sin(\alpha) = Acp, \qquad (8)$$

the formula for the static value of the reaction is obtained:

$$R_o = A(k^2 + c^2p^2)^{1/2}, \qquad (9)$$

If it is additionally taken into account that:

$$\text{tg}(\alpha) = \frac{cp}{k}, \qquad (10)$$

$$\text{tg}(\varphi) = \frac{cp}{k - mp^2}, \qquad (11)$$

the final dependency on the effectiveness of vibration isolation will be obtained in the form:

$$E_F = \frac{[F(t)]_{max}}{[R(t)]_{max}} = \frac{F_o}{A\sqrt{k^2 + c^2p^2}} = \sqrt{\frac{(k - mp^2)^2 + c^2p^2}{k^2 + c^2p^2}} = \sqrt{\frac{(1 - \delta^2)^2 + 4\xi^2\delta^2}{1 + 4\xi^2\delta^2}}, \qquad (12)$$

where:
ξ − non-dimensional attenuation coefficient.

The assessment of the effectiveness of vibration isolation depends on the susceptibility of the machine and the foundation (a primary connection) and on the direct and cross-impact susceptibility of the isolator.

Displacement vibration isolation (Fig. 3) requires obtaining a vibration protection to a system with a susceptibility matrix β located on a foundation with properties δ. The source of forcing determines the vibrations of the foundation.
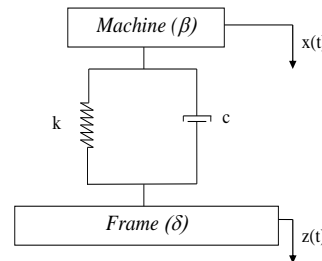

Fig. 3. Definition of a displacement vibration isolation [12]

The value of displacements transferred to the engine frame structure in displacement vibration isolation should be much smaller than the values obtained as a result of excitations from dynamic processes occurring in the facility:

$$Ampl[x(t)] \ll Ampl[z(t)], \qquad (13)$$

The equation describing the dynamic interactions for a system with displacement vibration isolation is described by the following relationship:

$$m\frac{d^2x}{dt^2} + c\left(\frac{dx}{dt} - \frac{dz}{dt}\right) + k(x - z) = 0, \qquad (14)$$

As a result of transforming the above equation, an equation describing the value of displacements using a vibroisolator is obtained:

$$z(t) = z_o(k\cos(pt) - cp\sin(pt)) = z_o\sqrt{k^2 + c^2p^2}\cos(pt + \alpha), \qquad (15)$$

where:

$z_o(t)$ – displacement of a system after a vibration vibroisolator in the conditions of a static force.

Taking into account this relationship allows you to obtain a formula for the effectiveness of displacement vibration isolation:

$$E_x = \frac{[z(t)]_{max}}{[x(t)]_{max}} = \frac{\sqrt{(k-mp^2)^2+c^2p^2}}{\sqrt{k^2+c^2p^2}}, \qquad (16)$$

The mathematical relationships obtained for the force and displacement vibration isolations are equal. When there is a force isolation on a rigid foundation, it is equivalent to the displacement isolation for a kinematic forcing. Dynamic properties of the component systems are undoubtedly important in the isolation process. Systems have passive elements in which the vibration isolator is a symmetrical mechanical system in the case of no energy being added from outside (properties of the vibration isolator are elastic for low frequencies). Dynamic characteristics of the machine and foundation should be used in the above assessment. The above point measures can also be obtained based on empirical research. The susceptibility of the isolator also depends on the frequency. The issues of vibration isolation of systems require further detailed studies and empirical research, especially in the context of the development of materials engineering [1, 15, 17, 18, 23, 25, 27].

2. METHODOLOGICAL BASIS OF RESEARCH

The assessment of the quality of vibration isolation was carried out based on an empirical experiment, enabling the most faithful reflection of the dynamics of the system and its degree of damping in the case of vibroacoustic energy dissipation. The study focused on a passive experiment (without external influences). The efficiency of damping the dynamic forces of the combustion engine at the test stand is a measure of the physical quantities used to describe it. Therefore, physical quantities were used as diagnostic parameters enabling a physical interpretation between a change in the system state and a change in the parameter value. The description of the transformation occurring in the object or the properties of the system after it occurred using this physical quantity constituted the basis of the developed methodology.

A four-cylinder internal combustion piston engine used in aviation, characterized by a specific set of physical quantities and relations between them, was selected as the research object. The aim of the research was to determine the values of the amplitudes and vibroacoustic energy generated as a result of dynamic processes in the research object for the case without and with the use of vibroisolation. Thanks to this, it was possible to quantify the effectiveness of the mechanical vibration damping process for specific measurement points and engine operating conditions. The change in dynamics was implemented by changing the engine speed, the values and number of which were selected from the useful range of the object's operating speed. For a given speed, vibration acceleration measurements were made on the engine block and engine frame.

For both locations of the measurement points, vibration accelerations were recorded in three perpendicular directions. Triaxial vibration transducers were located closest to the area of action of the resultant dynamic force, both for its original amplitude and in the damping area. Thanks to this, it was possible to build specific functional relations in order to determine the efficiency of vibration damping using a specific type of vibration isolation. Three directions of recording vibration parameters, which were: X – parallel to the cylinder axis (and perpendicular to the frame surface), Y – parallel to the frame surface and perpendicular to the crankshaft axis, Z – parallel to the crankshaft axis and perpendicular to the cylinder axis, allowed to indicate the dimension with the greatest dynamics and unambiguity of changes with changes in the source process. The assessment was carried out for both displacements, velocities and vibration accelerations.

The test conditions were characterized by the stability of the control vector, thanks to which the constant value of a rotational speed was maintained at a given engine operating point. The higher rotational speed was accompanied by an increase in the amplitude and energy value of the vibroacoustic process, enabling verification of the correctness of the vibration isolation for a wide field of changes in the system's input parameters. Discrete values of vibration accelerations were recorded in parallel for a frequency response of 25.4 kHz while maintaining the thermodynamic stability of the test object. Analyzes of the research material were carried out using proprietary tools developed in the Bruel&Kjær and Matlab environments, and the selection of the impulse and energy vibroacoustic measures provided the basis for further verification of the correctness of the use of the vibroisolator of a given design and damping material installed at the test bench of an aircraft piston engine.

3. TEST BENCH AND RECORDING DEVICES

Vibration measurements were carried out in stationary conditions on the test stand presented in Fig. 4–5.

The research was performed using a B&K LAN-XI type 3050-A-060 card (parallel recording with a band frequency of up to 51.2 kHz) – Table 1, Fig. 5.

Measurement signals, recorded in parallel, were monitored in real time thanks to Pulse Reflex Core. Two B&K 4504A transducers (Table 2) enabled the measurement of vibration accelerations on the engine and the supporting structure. The above accelerometers were calibrated for each measurement axis separately, and high sensitivity, wide operating range and high resonance frequency as well as low sensitivity to

external factors enabled faithful reproduction of dynamic processes in the obtained time courses.

Fig. 4. Components of the measuring stand: 1 – computer, 2 – throttle and choke levers, 3 – desktop, 4 – air filter, 5 – oil tank, 6 –starter, 7 – regulator, 8 – magnetos, 9 – oil pressure gauge, 10 – oil cooler, 11 – water brake, 12 – coolant radiator, 13 – battery, 14 – main power switch, 15 – electromagnet, 16 – fuel tank
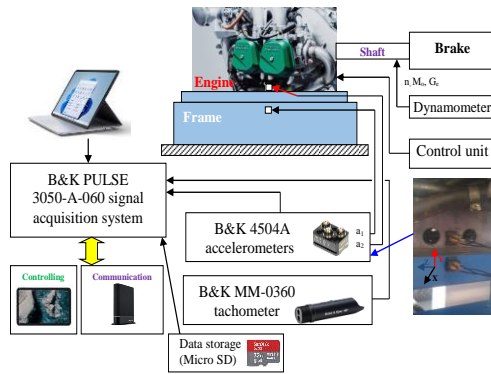

Fig. 5. Elements of the measurement path and the place of mounting the transducers

Table 1. Technical data of a LAN-XI 3050-A-060 [5]

Type of data	Value
Number of channels	6
Frequency passband [Hz]	1–51200
DC input [V DC]	10–32
Work temperature [ºC]	-25–70
Absolute amplitude precision, 1 kHz, 1 Vinput	±0.05 dB, typically ±0.01 dB
Linearity of an amplitude	±0.01–0.02 dB (from 0–140 dB)
Output	CCLD/microphone pre-amplifier (0 or 200 V polarization voltage), charge
Data handling	16 GB SD card (parallel recording at 25.6 kHz bandwidth)

Vibration acceleration signals were recorded on the engine block and engine frame, closest to the generated dynamic processes in the facility. For both locations, the signals were measured in three mutually perpendicular directions. Clear definition of each thermodynamic process in an aircraft engine was achieved using an angle encoder B&K MM0360 (Table 3).

Table 2. Technical data of a Bruel&Kjær 4504A transducer [6]

Type of data	Value
Frequency [Hz]	1–10000
Senitivity [mV/g]	10
Working temperature [ºC]	-50–125
Residual noise level in Spec. Freq. Range (RMS) [mg]	± 0.4
Maximum operational/shock level (peak) [g]	± 750/± 3000
Resonance frequency [kHz]	50
Triaxial/TEDS/Connector	Yes/No/10-32 UNF

Table 3. Technical data of the B&K MM0360 encoder [7]

Feature	Value
Range of velocity [rpm]	0–300000
Operating range	1.5 (0.6) to > 70 cm (27") and > 30º from centre line
Laser spot	< ∅5 mm at 70 cm distance
Maximum continuous input voltage [V]	–5 to +30
Laser class	3R. Visible 660–690 nm, CW, P [optical] < 2mW. Complies with EN/IEC 60825–1: 2007
Working temperature [ºC]	–10 to +50
Input type	CCLD (DeltaTron or ICP® inputs from 3 to 20 mA), U ≥ 20V

4. OBJECT DESCRIPTION

The Rotax 912 engine was selected as a research object in which the resultant dynamic force was generated from thermodynamic and mechanical processes, both main and accompanying. This object is a naturally aspirated, spark-ignition, internal combustion engine. The four-cylinder design is characterized by a counter-rotating arrangement of cylinders, in which there are two carburetors with a central fuel chamber (supplied by a mechanical fuel pump), and the pressure lubrication system (with the so-called dry sump) has 2 oil pumps and an oil cooler.

The Rotax 912 engine has a mixed cooling system: the cylinders are cooled by air and the heads by liquid (the liquid pump is driven by a gear transmission from the crankshaft). Each head is equipped with two hydraulically controlled valves, with the possibility of adjusting valve clearances (Fig. 6, Table 4). The engine is equipped with propeller speed reduction gearbox $i = 2.27$.

Fig. 6. View of the Rotax 912 engine [9]

Table 4. Technical data of the Rotax 912 engine [8]

Parameter type	Value
Rated effective power [kW]	59.6 (at 5800 rpm)
Maximum torque [N·m]	103 (at 4800 rpm)
Engine displacement [cm^3]	1211
Cylinder diameter/piston stroke [m/m]	0.0795/0.0610
Compression ratio [-]	9.1
Fuel consumption [dm^3/h]	15.0 (by 5000 rpm in 75% of rated effective power)
Mass power coefficient [kW/kg]	0.98
Engine length/width [m/m]	0.561/0.576

5. CONDITIONS OF EMPIRICAL STUDIES

Vibration insulation assessment tests of the tested engine were carried out under the following conditions:
- operating conditions: stationary, for each constant engine speed values and for a constant torque (7 engine speed values from the range 1600–3100 rpm) and the torque values were 0 N·m (Table 5),
- values of a torque for each engine speed was T = 0 N·m (to investigate only the effect of rotational speed changes on vibroisolation factors),
- vibroacoustic conditions: vibration acceleration passband range: 24 kHz,
- placement of a vibration transducer: first on the engine block (recording in the 3 perpendicular directions) and second at the engine frame (3 perpendicular directions),
- ambient conditions at the engine test stand area: t_o = 20 [^{o}C] and p_o = 1012 [hPa].
- Vibroacoustic signals obtained from the engine and the frame of the supporting structure were directed to the parallel inputs of the data acquisition card. The set of signals was subjected to analog and digital filtering, which were then saved in the mass memory of the recording unit. In the next stage, the process of time selection of the obtained waveforms was carried out,

thanks to which appropriate representative time sections were obtained that contained individual dynamic processes. The rotational speed parameter was obtained through the signal obtained from the angle encoder located behind the reducer, thanks to which the rotational speed on the engine crankshaft was calculated.

Table 5. Engine research conditions and recorded vibroacoustic parameters

Engine parameters	Recorded accelerations on engine	
n [rpm]	Block	Frame
1600		
2100		
2300	$a_{x, block}$	$a_{x, frame}$
2500	$a_{y, block}$	$a_{y, frame}$
2700	$a_{z, block}$	$a_{z, frame}$
2900		
3100		

6. RESULTS AND ANALYSIS

6.1. Assessment of the effectiveness of vibration isolation of the engine mounting

The quality of the selection of vibration isolating elements can be assessed by measuring vibration signals before and after the vibration isolator. Figure 7 shows the time history of vibration acceleration signals recorded on the engine and on the test stand frame in the X direction, while the time history of vibration acceleration signals recorded on the engine and on the test stand frame in the Y direction is shown in the Figure 8.

It can be concluded, based on the analysis of the Figure 7 and Figure 8, that the maximum vibration acceleration amplitudes have decreased for both directions of a vibration measurement. The vibration acceleration signals were analyzed by calculating the damping coefficient based on the equation [16]. The results of an analysis regarding the maximum vibration acceleration values are presented in the Table 6.

Table 7 presents the results of analyzes regarding vibration damping in the energetic sense, based on the root mean square values of vibration accelerations.

Based on the analysis of the damping coefficients listed in the Table 6 and Table 7, it was found that for all engine operation settings during the tests, the vibration acceleration signals were damped. Figure 9 shows the time history of vibration acceleration signals registered on the engine and on the test stand frame in the X direction, while the time history of vibration acceleration signals registered on the engine and on the test stand frame in the Y direction is shown in the Figure 10.
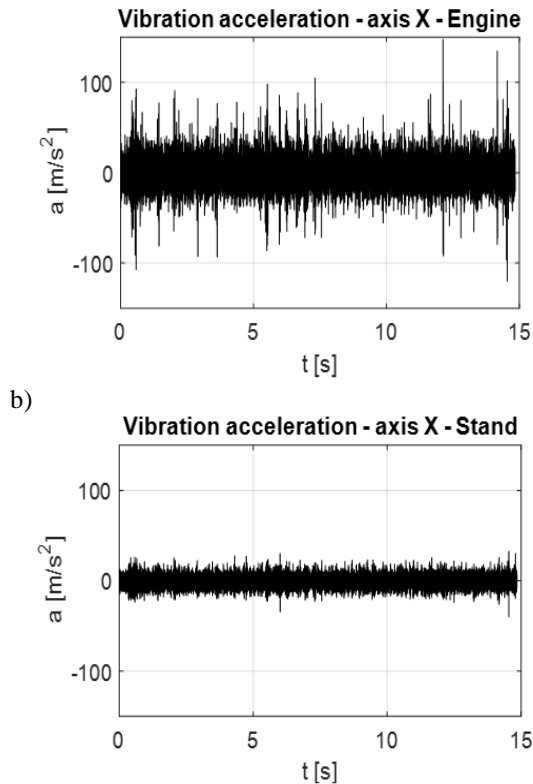
Fig. 7. The time history of vibration accelera-
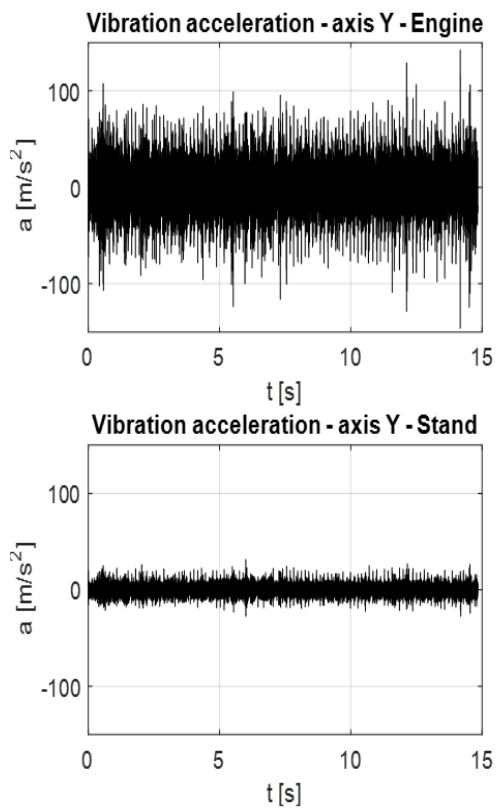tion for two measurement points in the direc-
tion X

b)

Fig. 8. The time history of vibration accelera-
tion for two measurement points in the direc-
tion Y

Table 6. Damping coefficients of vibration acceleration
signal parameters regarding maximum values

RPM	Vibration acceleration damping [dB/ref. 1μm/s²]	
	X axis	Y axis
1600	11.4	13.3
2100	10.8	13.4
2300	12.7	15.8
2500	8.7	13.8
2700	8.9	9.4
2900	10.8	15.6
3100	9.6	10.3

Table 7. Damping coefficients of vibration acceleration
signal parameters relating to the energy

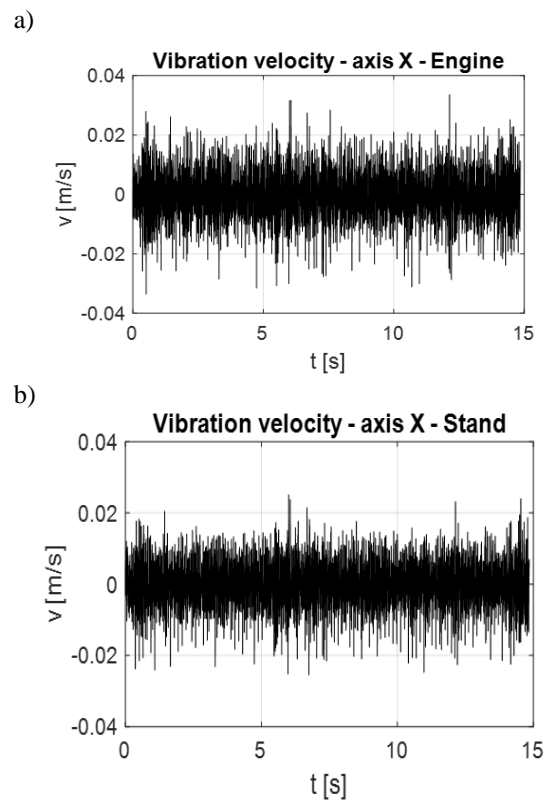| RPM	Vibration acceleration damping [dB/ref. 1μm/s²]	
	X axis	Y axis
1600	5.2	11.1
2100	5.3	11.1
2300	7.4	13.6
2500	7.1	10.8
2700	6.9	11.8
2900	6.4	12.2
3100	7.1	8.6

a)

b)

Fig. 9. The time history of vibration velocity
for two measurement points in the direction X

It can be concluded, based on the analysis of the Figure 9 and Figure 10, that the maximum vibration velocity amplitudes were reduced in the X direction, while they were strengthened in the Y direction. The vibration velocity signals were analyzed by calculating the damping coefficient. The results of an analysis regarding the maximum vibration acceleration values are presented in the Table 8.
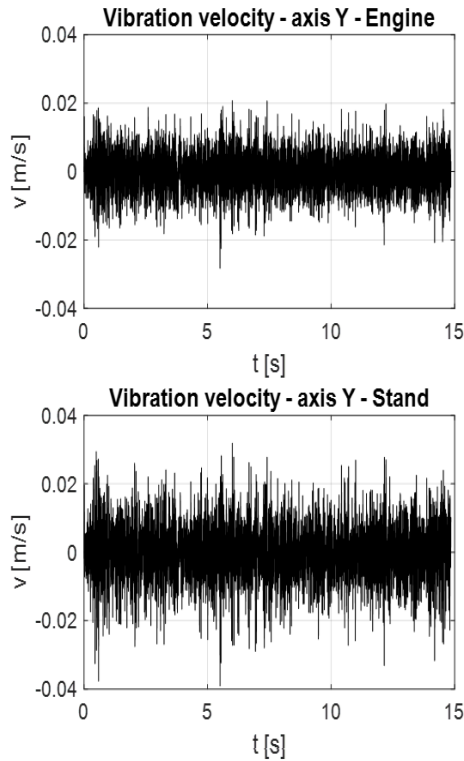

Fig. 10. The time history of vibration velocity for two measurement points in the direction Y

Table 8. Damping coefficients of vibration velocity signal parameters regarding maximum values

RPM	Vibration velocity damping [dB/ref. 1nm/s]	
	X axis	Y axis
1600	2.4	-2.8
2100	1.7	-3.8
2300	2.0	-2.6
2500	2.7	-4.8
2700	0.1	-2.8
2900	2.7	-3.7
3100	2.4	-3.6

Table 9 presents the results of analyzes regarding vibration damping in the energetic sense, based on the root mean square values of vibration velocities.

Basing on the analysis of the damping coefficients listed in the Table 8 and Table 9, it was found that for all engine operation settings during the tests, the vibration speed signals were damped in the X direction and strengthened in the Y direction. In a similar way,

the effectiveness of damping vibration displacements was analyzed, the time history of which is presented in the Figure 11 and Figure 12.

Table 9. Damping coefficients of vibration velocity signal parameters relating to the energy

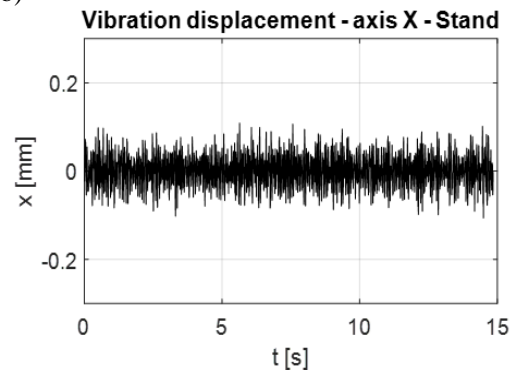| RPM	Vibration velocity damping [dB/ref. 1nm/s]	
	X axis	Y axis
1600	2.2	-4.4
2100	2.5	-5.6
2300	1.6	-4.1
2500	2.6	-5.3
2700	1.5	-3.2
2900	2.7	-3.7
3100	2.2	-4.2

a)
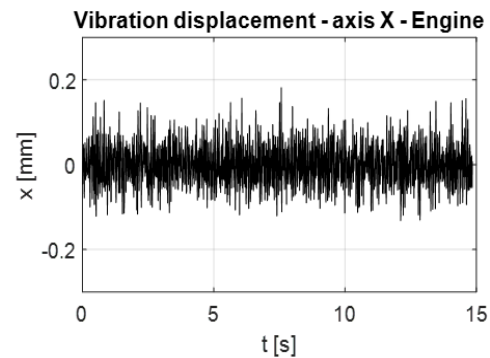
b)

Fig. 11. The time history of vibration displacement for two measurement points in the direction X

It was found, analyzing of the Figure 11 and Figure 12, that the maximum amplitudes of vibration displacements were reduced for the X direction, and strengthened for the Y direction. The vibration displacement signals were analyzed by calculating the damping coefficient. The results of the analyzes regarding the maximum values of vibration acceleration are presented in the Table 10, and the results of calculations regarding vibration damping in the energetic sense, based on the root mean square values of vibration velocities, are presented in the Table 11.

Vibration displacement - axis Y - Engine

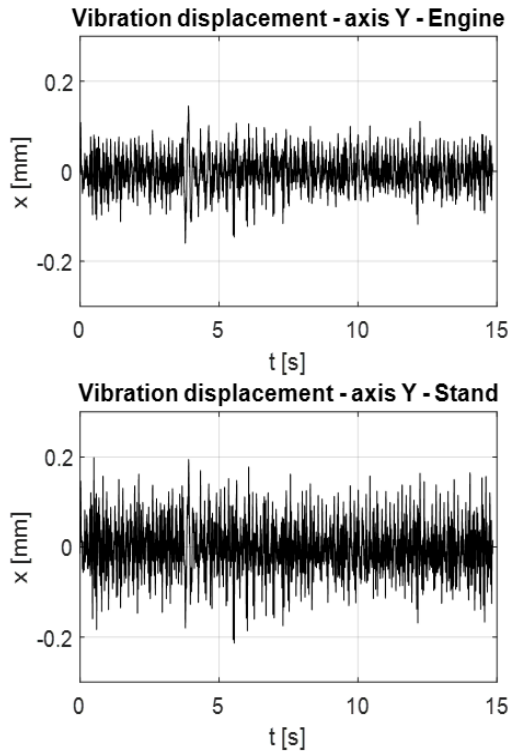**Vibration displacement - axis Y - Stand**

Fig. 12. The time history of vibration displacement for two measurement points in the direction Y

Table 10. Damping coefficients of vibration displacement signal parameters regarding maximum values

RPM	Vibration displacement damping [dB/ref. 1pm]	
	X axis	Y axis
1600	4.4	-2.5
2100	3.5	-4.0
2300	2.9	-1.8
2500	4.7	-3.0
2700	4.2	-3.5
2900	5.6	-5.1
3100	4.0	-5.0

Basing on the analysis of the damping coefficients listed in the Table 10 and Table 11, it was found that for all engine operating settings during the tests, the vibration displacement signals were damped in the X direction and strengthened in the Y direction.

6.2. Order analysis

The results of the broadband analysis were ambiguous, therefore an order analysis was performed to explain the discrepancies between the results of the calculated damping coefficients for accelerations, velocities and vibration displacements, especially in the Y direction. Table 12 shows the assignment of order numbers to dynamic phenomena occurring in the combustion engine.

Table 11. Damping coefficients of vibration displacement signal parameters relating to the energy

RPM	Vibration displacement damping [dB/ref. 1pm]	
	X axis	Y axis
1600	2.5	-3.3
2100	1.9	-4.2
2300	1.1	-3.2
2500	2.4	-4.8
2700	2.3	-3.6
2900	4.3	-4.6
3100	5.3	-5.5

Figures 13 and 14 present the order analysis for vibration acceleration signals recorded in two perpendicular directions. The waveforms were presented for a speed of 1600 rpm, reflecting the lowest value of energy generated in the source process converted into the vibration process (verification of effectiveness for the most sensitive working conditions − the lowest possible values of vibration isolation effectiveness).

Table 12. Assignment of the order number to dynamic phenomena occurring in the combustion engine

Type of a vibration source	Order
Imbalance of the masses of the piston-crank system performing rotation	1
	2
	3
Imbalance of the masses of the piston-crank system performing back-and-forth motion	2
	4
	6
Ignition frequency	2
	4
	6
Ignition frequency of a one cylinder	0.5
	1
	1.5

It can be concluded, based on the analysis of the results presented in the Figure 13 and Figure 14, that for the X direction, damping occurs for orders no greater than 2, while for higher orders an amplification of vibrations is observed. Damping was not observed for all rows for the Y direction,. The coefficients describing the damping of vibration accelerations for orders kinematically related to dynamic phenomena in the combustion engine are included in the Table 13.

The order analysis for vibration velocity signals recorded in two perpendicular directions is presented in the Figure 15 and Figure 16.
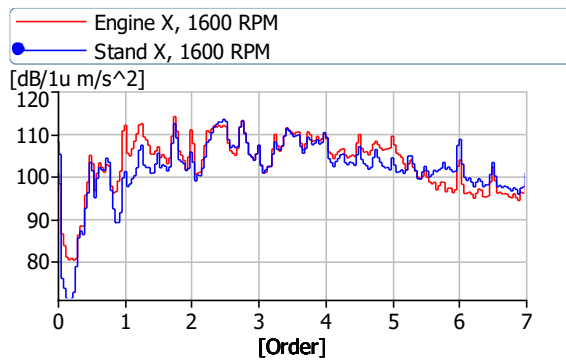
Fig. 13. The order characteristics of a vibration acceleration for two measurement points in the direction X
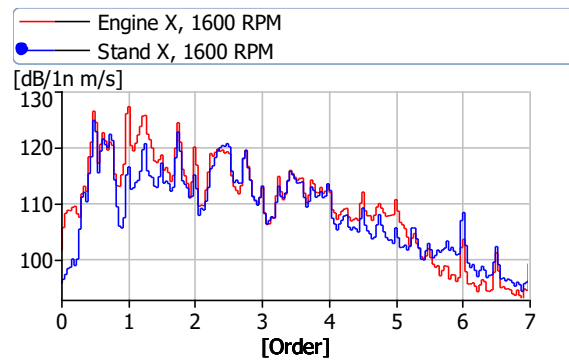

Fig. 15. The order characteristics of a vibration velocity for two measurement points in the direction X
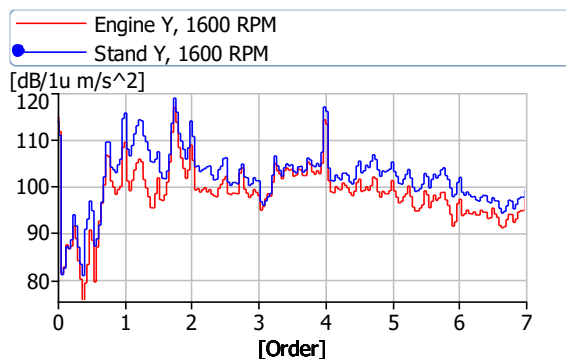

Fig. 14. The order characteristics of a vibration acceleration for two measurement points in the direction Y
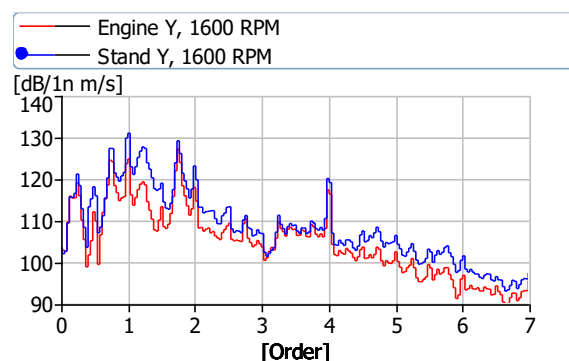

Fig. 16. The order characteristics of vibration velocity for two measurement points in the direction Y

Table 13. List of damping (vibration accelerations) coefficients for orders kinematically related to dynamic phenomena in an internal combustion engine

Order	Vibration acceleration damping [dB/ref. $1\mu m/s^2$]	
	X axis	Y axis
0.5	1.7	-6
1	10	-6
1.5	2	-5
2	6	-3
3	0	-3
4	0	-3
6	-5	-6

Table 14. List of damping coefficients (vibration velocities) for orders kinematically related to dynamic phenomena in an internal combustion engine

Order	Vibration velocity damping [dB/ref. 1nm/s]	
	X axis	Y axis
0.5	2	-6
1	10	-7
1.5	3	-6
2	5	-5
3	0	-3
4	0	-3
6	-5	-5

Basing on the analysis of the results presented in the Figure 15 and Figure 16, it can be concluded that, for the X direction, damping occurred for orders no greater than 2, while for higher orders an amplification of vibrations was observed. Damping also occurred for order 5, which was not kinematically related to the phenomena in the engine. For the Y direction, no damping was observed for all orders. The coefficients describing the vibration velocity damping for orders kinematically related to dynamic phenomena in the combustion engine are included in the Table 14.

Figure 17 and Figure 18 present the order analysis for vibration displacement signals recorded in two perpendicular directions.

It can be concluded, based on the analysis of the results presented in the Figure 17 and Figure 18, that for the X direction, damping occurred for orders no greater than 2, while for higher orders an amplification of vibrations was observed. Damping also occurred for order 5, which was not kinematically related to the phenomena in the engine. For the Y direction, no damping was observed for all rows. The coefficients describing the damping of vibration accelerations for orders kinematically related to dynamic

phenomena in the combustion engine are included in the Table 15.
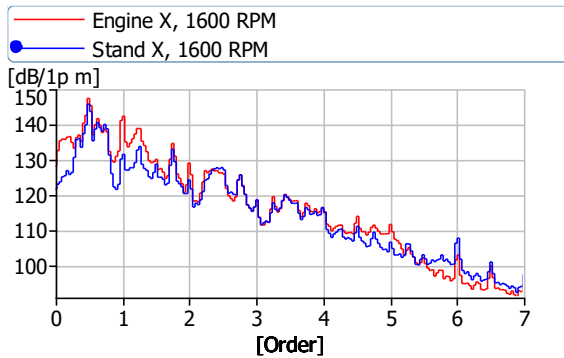

Fig. 17. The order characteristics of a vibration displacement for two measurement points in the direction X
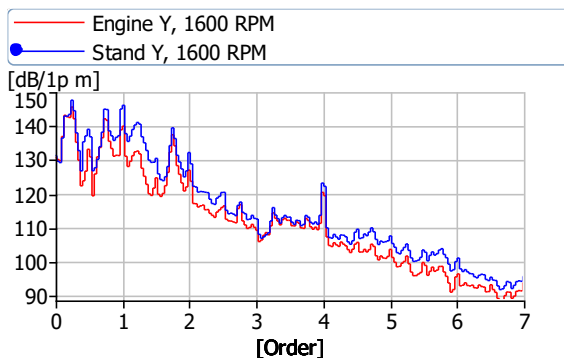

Fig. 18. The order characteristics of a vibration displacement for two measurement points in the direction Y

Table 15. List of damping coefficients (vibration displacements) for orders kinematically related to dynamic phenomena in an internal combustion engine

Order	Vibration displacement damping [dB/ref. 1pm]	
	X axis	Y axis
0.5	2	-6
1	11	-6
1.5	2	-6
2	5	-6
3	0	-2
4	0	-3
6	-5	-5

7. CONCLUSIONS

Scientific issues related to the design, manufacture and empirical verification of the correctness of the foundation of research facilities on their test stands, taking into account the criterion of minimizing dynamic impacts arising from the processes implemented in them, they are in line with contemporary research directions in the area of designing and operation of systems for the production and conversion of energy into mechanical work. The authors of this work undertook such a task, focusing on a stand for testing aircraft engines, in this case an internal combustion piston engine of this category.

The subject of the research was the assessment of damping effectiveness, which was carried out in empirical studies using point measures of vibroacoustic processes of impulse and energy natures, such as the peak value and RMS. The above effectiveness was assessed using the damping coefficient for the X and Y directions at different engine speeds, for which high damping effectiveness for vibration accelerations was confirmed. The analysis of the degree of damping for the vibration speeds showed a reduction in the vibration amplitude for the peak and RMS values only in the case of the X direction The same relations were observed for vibration displacements, hence order analysis was additionally used as a tool for more precise observation of functional relations in the set of vibroacoustic parameters.

Based on the results obtained from the order analysis, it was found that: for vibration acceleration signals measured in the X direction, damping occurs for orders no larger than 2. For the Y direction, no damping was observed for all orders. In the case of measuring of vibration velocities and displacements in the X direction, damping occurs for orders no greater than 2, while for higher orders, vibration amplification is observed. Damping also occurs for the order 5, which is not kinematically related to the phenomena in the engine. For the Y direction, no damping was observed for all orders.

It can be concluded, based on the presented research material, that the applied vibroisolators effectively dampen high-frequency vibrations. Their effectiveness for vibrations in the X direction is limited to the first two orders, while in the Y direction they cause amplification of vibrations.

Author contributions: *research concept and design, G.M.S., M.M.; Collection and/or assembly of data, G.M.S., M.M.; Data analysis and interpretation, G.M.S., M.M.; Writing the article, G.M.S., M.M., W.M.; Critical revision of the article, G.M.S., M.M., W.M.; Final approval of the article, G.M.S., M.M., W.M.*

Declaration of competing interest: *The authors declare that they have no known competing financial interests or personal relationships that could have appeared to influence the work reported in this paper.*

REFERENCES

1. Cao Y, Peng P, Wang H, Sun J, Xiao G, Zuo Z. Development of an innovative three-dimensional vibration isolation bearing. Engineering Structures 2023; 295: 116890. https://doi.org/10.1016/j.engstruct.2023.116890.
2. Divijesh PP, Rao M, Rao R, Jain N, Prabhu P. Implementation of structurally pre-stressed piezo actuator

based active vibration isolation system for micro milling. Materials Today: Proceedings 2023; 92: 182–8.

3. Fang S, Chen K, Zhao B, Lai Z, Zhou S, Liao WH. Simultaneous broadband vibration isolation and energy harvesting at low frequencies with quasi-zero stiffness and nonlinear monostability. Journal of Sound and Vibration. 2023;553:117684.
https://doi.org/10.1016/j.jsv.2023.117684.

4. Fiebig W, Wróbel J. Two stage vibration isolation of vibratory shake-out conveyor. Archives of Civil and Mechanical Engineering 2017; 17(2): 199–204.
https://doi.org/10.1016/j.acme.2016.10.001.

5. https://www.bksv.com/en/instruments/daq-data-acquisition/lan-xi-daq-system/daq-modules/type-3050
(access date: 07.05.2024).

6. https://www.bksv.com/en/transducers/vibration/accelerometers/ccld-iepe/4504-a (access date: 07.05.2024).

7. https://www.bksv.com/media/doc/bp2288.pdf
(access date: 07.05.2024).

8. https://www.flyrotax.com/pl/products/912-ul-a-f
(access date: 07.05.2024).

9. https://www.lockwood.aero/engine-details/rotax-912uls/314 (access date: 07.05.2024).

10. Idaszewska N, Szymański GM. Identification of Characteristic Vibration Signal Parameters During Transport of Fruit and Vegetable. Vibrations in Physical Systems; 2020; 31(1): 2020111-1 2020111-10.

11. Kobaszyńska-Twardowska A, Krzyżanowski M, Siwka P. Forecasting Trends of Safety Performance Indicators in Aviation. Safety & Defense 2023; 9(2): 1–11.
https://doi.org/10.37105/sd.201.

12. Korbicz J, Kościelny J. Modeling, diagnostics, and mastering processes. DiaSter implementation. Scientific and Technical Publishing House, Warsaw 2010.

13. Liu C, Yu K, Liao B, Hu R. Enhanced vibration isolation performance of quasi-zero-stiffness isolator by introducing tunable nonlinear inerter. Communications in Nonlinear Science and Numerical Simulation 2021; 95: 105654. https://doi.org/10.1016/j.cnsns.2020.105654.

14. Liu H, Huang X, Ding P, Wang B. Reliability evaluation method of vibration isolation performance of nonlinear isolator. Journal of Sound and Vibration 2023; 551:117616.
https://doi.org/10.1016/j.jsv.2023.117616.

15. Liu S, Peng G, Li Z, Li W, Sun L. Low-frequency vibration isolation via an elastic origami-inspired structure. International Journal of Mechanical Sciences 2023;260:108622.
https://doi.org/10.1016/j.ijmecsci.2023.108622.

16. Lu JJ, Yan G, Qi WH, Yan H, Shi JW, Chen A, i in. Load-adaptive quasi-zero stiffness vibration isolation via dual electromagnetic stiffness regulation. Journal of Sound and Vibration 2023; 567: 118059.
https://doi.org/10.1016/j.jsv.2023.118059.

17. Palacio O, Malfait WJ, Michel S, Barbezat M, Mazrouei-Sebdani Z. Vibration and structure-borne sound isolation properties of silica aerogels. Construction and Building Materials 2023; 399: 132568.
https://doi.org/10.1016/j.conbuildmat.2023.132568.

18. Palmić TB, Slavič J. Single-process 3D-printed stacked dielectric actuator. International Journal of Mechanical Sciences 2022; 230: 107555.
https://doi.org/10.1016/j.ijmecsci.2022.107555.

19. Song H, Shan X, Hou W, Wang C, Sun K, Xie T. A novel piezoelectric-based active-passive vibration isolator for low-frequency vibration system and experimental analysis of vibration isolation performance. Energy. 2023;278:127870.
https://doi.org/10.1016/j.energy.2023.127870.

20. Tian Y, Cao D, Chen C, Zhang X. Vibration isolation performance of a rectangular panel with high-static-low-dynamic stiffness supports. Applied Mathematical Modelling 2023; 119: 218–38.
https://doi.org/10.1016/j.apm.2023.02.027.

21. Waligórski M, Batura K, Kucal K, Merkisz J. Empirical assessment of thermodynamic processes of a turbojet engine in the process values field using vibration parameters. Measurement 2020; 158: 107702.
https://doi.org/10.1016/j.measurement.2020.107702.

22. Waligórski M, Batura K, Kucal K, Merkisz J. Research on airplanes engines dynamic processes with modern acoustic methods for fast and accurate diagnostics and safety improvement. Measurement 2020; 154: 107460.
https://doi.org/10.1016/j.measurement.2019.107460.

23. Waśniewski G, Schabowicz K, Wróblewski K, Kasprzak T. Identification of physical model of resinous material filling expansion joint in reinforced concrete structures. Journal of Building Engineering 2022; 45:103505.
https://doi.org/10.1016/j.jobe.2021.103505.

24. Xie X, He P, Wu D, Zhang Z. Ultra-low frequency active vibration isolation in high precision equipment with electromagnetic suspension: Analysis and experiment. Precision Engineering 2023; 84: 91–101.
https://doi.org/10.1016/j.precisioneng.2023.07.004.

25. Yu R, Rui S, Wang X, Ma F. An integrated load-bearing and vibration-isolation supporter with decorated metamaterial absorbers. International Journal of Mechanical. Sciences 2023; 253: 108406.
https://doi.org/10.1016/j.ijmecsci.2023.108406.

26. Zhang C, He J, Zhou G, Wang K, Xu D, Zhou J. Compliant quasi-zero-stiffness isolator for low-frequency torsional vibration isolation. Mechanism and Machine Theory 2023; 181: 105213.
https://doi.org/10.1016/j.mechmachtheory.2022.105213.

27. Zhao J, Zhou G, Zhang D, Kovacic I, Zhu R, Hu H. Integrated design of a lightweight metastructure for broadband vibration isolation. International Journal of Mechanical Sciences 2023; 244: 108069.
https://doi.org/10.1016/j.ijmecsci.2022.108069.

Grzegorz M. SZYMAŃSKI
professor in the Faculty of Civil and Transport Engineering (Institute of Transport) at the Poznan University of Technology, Poland.
Contact: grzegorz.m.szymanski@put.poznan.pl

Wojciech MISZTAL
 doctor in the Faculty of Civil and Transport Engineering (Institute of Transport) at the Poznan University of Technology, Poland.
Contact:
wojciech.misztal@put.poznan.pl

Marek WALIGÓRSKI - professor in the Faculty of Civil and Transport Engineering (Institute of Combustion Engines and Powertrains) at the Poznan University of Technology, Poland.
Contact:
marek.waligorski@put.poznan.pl